Citation (APA)
Balci, E., García, P. V., Alcalde, M., & Hollmann, F. (2026). H_2O_2-driven enzymatic degradation of halophenols and toxicity assessment. *Environmental Technology and Innovation*, *42*, Article 104923.
https://doi.org/10.1016/j.eti.2026.104923

Environmental Technology & Innovation 42 (2026) 104923

Contents lists available at ScienceDirect

Environmental Technology & Innovation

journal homepage: www.elsevier.com/locate/eti

H_2O_2-driven enzymatic degradation of halophenols and toxicity assessment

Esin Balci [a,b,*], Pablo Velázquez García [a,**], Miguel Alcalde [c], Frank Hollmann [a]

[a] Delft University of Technology, Department of Biotechnology, Van der Maasweg 9, Delft 2629 Hz, the Netherlands
[b] Izmir Institute of Technology, Faculty of Engineering, Department of Environmental Engineering, Urla, İzmir 35430, Türkiye
[c] Department of Biocatalysis, Institute of Catalysis, CSIC, Madrid 28049, Spain

ARTICLE INFO

Keywords:
Halophenols
Enzymatic degradation
Unspecific peroxygenase
Priority pollutants
Environmental remediation

ABSTRACT

Halophenols (HPs) cause serious problems for the health of living beings and environment due to their toxigenicity, mutagenicity and carcinogenicity. Enzymes have recently attracted significant attention as an eco-friendly and sustainable approach for the environmental remediation of pollutants. In this study, the recombinant unspecific peroxygenase from *Agrocybe aegerita* (r*Aae*UPO, recombinantly expressed in *Komagataella pastoris* known as *Pichia pastoris*) was used to degrade five representative HPs (2-Chlorophenol (2-CP), 3-Chlorophenol (3-CP), 4-Chlorophenol (4-CP), 4-Bromophenol (4-BP), and 3-Iodophenol (3-IP)) in the batch and fed-batch systems. r*Aae*UPO (5 μM) completely removed up to 10 mM HPs from the fed-batch system in 48 h, while the almost complete removal of 2.5 mM 4-CP and 4-BP in batch systems occurred within 72 h. The enzyme was more effective upon slow, continuous fed with H_2O_2 concentrations (2 mM/h) than supplying stoichiometric H_2O_2 from the beginning. The activity of r*Aae*UPO towards HPs was: 3-IP > 2-CP > 3-CP > 4-BP > 4-CP. These results were also confirmed by molecular docking results. r*Aae*UPO-catalyzed primary degradation of HPs occurred via catechol formation followed by polymerization. Toxicity assays using *E. coli* DH5α demonstrated a significant reduction in toxicity after enzymatic degradation of HPs. This study revealed that r*Aae*UPO is an efficient biocatalyst capable of effectively degrading HPs, showing great potential for environmental bioremediation applications.

1. Introduction

Halophenols (HPs) are aromatic compounds derived from phenols with a halogen atom (chlorine, bromine, fluorine, and iodine) that exhibit high chemical stability and environmental persistence. They have been widely employed as flame retardants, refrigerants, disinfectants, additives, preservatives in a variety of industrial, agricultural, and household applications (Lu et al., 2015; Liu et al., 2020). Large quantities of HPs may enter the environment through industrial effluents, accidental releases, or excessive use of products containing these chemicals (Acero et al., 2005; Jiang et al., 2014; Lin et al., 2016). Their strong carbon–halogen bonds render them environmentally persistent, leading to accumulation in water, air, and soil. HPs are of major toxicological concern due to their mutagenic, carcinogenic, and endocrine-disrupting properties, as well as their acute toxicity to microorganisms and higher organisms

---

[*] Corresponding author at: Delft University of Technology, Department of Biotechnology, Van der Maasweg 9, Delft 2629 Hz, the Netherlands.
[**] Corresponding author.

E-mail addresses: esinbalci@iyte.edu.tr (E. Balci), pvelazquezgarcia@tudelft.nl (P.V. García).

https://doi.org/10.1016/j.eti.2026.104923
Received 26 November 2025; Received in revised form 12 March 2026; Accepted 2 April 2026

(Pera-Titus et al., 2004; Wang et al., 2021). Several HPs, including chlorophenols (CPs) and bromophenols (BPs), are classified as priority pollutants by both the U.S. Environmental Protection Agency and European Union Legislation, owing to all these properties (Bagheri et al., 2004; Igbinosa et al., 2013). Thus, it is imperative to develop effective methods to eliminate HPs in contaminated environments.

Conventional treatment methods such as flocculation, chemical oxidation, adsorption, ion exchange, and reverse osmosis are often costly, inefficient, and environmentally unsound, frequently resulting in the production of secondary toxic by-products (Ra et al., 2008; Olaniran and Igbinosa, 2011). In contrast, biological degradation via microbial or enzymatic processes offers a more environmentally benign route. However, microbial approaches are often limited by the high toxicity of HPs and the slow kinetics of biodegradation. In this context, enzymatic catalysis represents a promising alternative for HP detoxification (Duran and Esposito, 2000). In literature, mono- and dioxygenases (Suma et al., 2016; Kang et al., 2017), phenol oxidases such as tyrosinases and laccases (Loncar et al., 2011; Lu et al., 2015; Davis et al., 2018; Jankowska et al., 2024), and peroxidases (Ashraf and Husain, 2010; Kim et al., 2012; Karich et al., 2017; De Boer et al., 2025) have been evaluated for the treatment of aromatic contaminants.

Unspecific peroxygenases (UPOs) are fungal extracellular enzymes suspected of being involved in fungal lignin-depolymerization (Hofrichter and Ullrich, 2014). The reactivity and exceptional robustness of the UPO from *Agrocybe aegerita* (*Aae*UPO) make it a prime candidate catalyst for the degradation of HPs (Ullrich et al., 2004). In previous studies, Karich et al. (2017) have qualitatively already demonstrated the versatility of *Aae*UPO. This provided a basis for conducting further investigation into the *Aae*UPO-catalyzed degradation of HPs. In this study, HPs' degradation was investigated using the recombinant, evolved variant of *Aae*UPO (Molina-Espeja et al., 2015) (r*Aae*UPO) produced on pilot-scale fermentation using recombinant *Komagataella pastoris* known as *Pichia pastoris*) (Tonin et al., 2021). Before and after enzymatic degradation, HPs' toxicity was assessed, measuring the inhibition of the growth rate of bacteria (*E. coli* DH5α). Moreover, by using molecular docking approaches, information about orientation and binding affinity of each HPs was obtained.

2. Materials and method

2.1. Materials

2-Chlorophenol (2-CP), 4-Bromophenol (4-BP), 3-Iodophenol (3-IP), as well as 4-Chlorocatechol (4-CC), 4-Bromocatechol (4-BC), 3-Iodocatechol (3-IC), and H_2O_2 (50% wt. in H_2O stabilized) were purchased from Sigma-Aldrich. 3-Chlorophenol (3-CP), 4-Chlorophenol (4-CP), and Sodium L-Ascorbate were obtained from TCI Chemicals. All chemicals were of analytical grade and utilized without any further purification.

2.2. Enzyme preparation

The enzyme preparation used in this study stems from a previous large-scale fermentation campaign (Tonin et al., 2021). To remove remaining *Pichia pastoris* cells, the crude enzyme solution was centrifuged at 10,000 × g for 30 min at 4 °C. The supernatant was passed through a 20 μm filter and stored at −80 °C until further use. For purification of r*Aae*UPO, a single passage over Q Sepharose FF (30 mL) column at a flow rate of 5 mL/min (NGC Chromatography system (Biorad)) was performed. Following the initial loading of 90 mL, the bound protein was eluted using a linear NaCl gradient: 0–50% over 450 mL, 50–100% over 50 mL, and finally 100% NaCl over an additional 75 mL. The activity in the collected fractions was assessed via the oxidation of 2,2′-azino-bis(3-ethylbenzothiazoline-6-sulfonic acid) (ABTS). Active fractions were pooled, concentrated using Amicon centrifugal filters with a 10 kDa molecular weight cut-off, and subsequently dialyzed against 50 mM sodium phosphate buffer (pH 7). The resulting r*Aae*UPO preparation was largely enriched (Fig. S1).

2.3. Enzyme activity measurement

The activity of r*Aae*UPO was determined using 2 mM ABTS in sodium citrate buffer at pH 4. The formation of the $ABTS^+$ radical was spectrophotometrically monitored for 3 min at 420 nm. One unit (U) of enzyme activity expresses the amount of enzyme catalyzing the formation of 1 μmol of $ABTS^+$ per 1 min under the assay conditions. Extinction coefficient of ABTS at 420 nm is 36 mM^{-1} cm^{-1}.

2.4. Enzyme concentration determination

Pierce bicinchoninic acid (BCA) Protein Test Kit (Advion Interchim Scientific) was utilized to determine the enzyme's protein content. Using the Bovine serum albumin as a standard protein, a calibration curve was formed. Based on the obtained equation, enzyme protein content was calculated.

2.5. CO difference spectra

r*Aae*UPO concentration was determined using carbon monoxide (CO)-difference spectra. The extinction coefficient at 445 nm was assumed to be 107 mM^{-1} cm^{-1} for *Aae*UPO. A total of 950 μL of the protein sample, diluted in 100 mM potassium phosphate (KPi) buffer at pH 7.5, was transferred into plastic cuvettes and placed in a Cary 60 spectrophotometer (Agilent). Following baseline correction, the sample was exposed to carbon monoxide for a few seconds. Subsequently, 50 μL of a 1 M sodium dithionite stock solution was added, and the absorbance spectrum between 400 and 500 nm was recorded. Measurements continued until a stable absorption signal was observed.

2.6. Enzymatic reaction

Reaction solutions (1 mL) were prepared with and without sodium ascorbate (NaAsc). For experiments to be performed using NaAsc, 15 mg of NaAsc was added into the plastic tubes to prevent polymerization. The stock solutions (100 mM) of 2-CP, 3-CP, 4-CP, 4-BP, and 3-IP were separately prepared in acetonitrile. 1 M H_2O_2 solution was prepared by diluting it (50% wt. in H_2O stabilized) with KPi buffer (50 mM, pH 7). The appropriate enzyme concentration was determined when the experiments were separately carried out using different enzyme concentration (0.1, 0.5, 1, 2.5, and 5 μM) at 30 °C and 600 rpm for 30 min. Furthermore, to determine the appropriate quantification of H_2O_2 in the reaction, various concentrations of H_2O_2 (1, 2, 3, 4, 5, 7.5, 10, 15, 20, 25, and 30 mM) were added to the reaction mixture (1 mL) containing 2.5 mM HPs, 5 μM r*Aae*UPO, 15 mg NaAsc, and KPi buffer. The experiments were performed in a thermomixer at 30 °C and 600 rpm for 4 h in triplicate. To observe the catalytic ability of the enzyme upon pollutant concentration, different concentrations of HPs (1, 2.5, 5, and 10 mM) were tested using the 5 μM r*Aae*UPO and 25 mM H_2O_2 concentration for 30 min. After the incubation period, all samples were put into an ice tube to terminate the reactions. To extract the HPs in the reaction mixture, 1 mL of ethyl acetate (v/v) was used for the GC and GC-MS analyses.

2.6.1. Enzymatic reaction in a batch system

Batch experiments were conducted in a plastic tube in triplicate. Each tube (1 mL) contained 25 μL of HP congener (100 mM), 20 μL of r*Aae*UPO (250 μM), 930 μL KPi buffer (50 mM, pH 7), and 25 μL H_2O_2 (1 M). The concentrations of HP congener and enzyme in the tubes were adjusted to be 2.5 mM and 5 μM, respectively. The tubes were held in the thermomixer at 30 °C and 600 rpm during 48 h. With the addition of H_2O_2, the enzymatic reaction was started. The control experiments were performed using H_2O_2 without enzyme under the same conditions within the same time period. At the end of incubation, to stop the reaction, the tubes were put in the ice bath. To extract the HPs and their metabolites in aqueous system, 1 mL of ethyl acetate was added into the samples (v/v) for the GC and GC-MS analyses. Once the obtained solution was vortexed and centrifuged at 15,000 rpm for 5 min, the supernatant phase was taken into the vial for further analysis.

2.6.2. Enzymatic reactions in a fed-batch system

Experiments were carried out in a thermomixer at 30 °C and 600 rpm for 72 h in triplicate. The reaction solution (10 mL) consisted of 1000 μL of HP congener (100 mM), 200 μL of r*Aae*UPO (250 μM), 8600 μL KPi buffer (50 mM, pH 7), and 200 μL H_2O_2 (100 mM). The reaction mixture with 10 mM HPs was fed with 2 mM H_2O_2/h using a pump. After the samples were collected from the system, the reaction tubes were put in the ice bath to terminate the reaction. For the GC and GC-MS analysis, 1 mL of ethyl acetate was added into the samples (v/v) so that the HPs and their metabolites in aqueous system were extracted. After the obtained solution was vortexed for 1 min and centrifuged at 15,000 rpm for 5 min, the supernatant phase was taken into the vial.

2.7. Molecular docking

The corresponding accession number (8AV5) of *Aae*UPO was obtained from RCSB protein databank AutoDock Vina in Chimera (1.19) and DockThor molecular docking programs were used to evaluate the binding affinity of *Aae*UPO to HPs in the presence of H_2O_2.

2.8. Toxicity experiments

Measurement of the pollutants' chemical toxicity is very important in the environment. Baek and An (2011) reported that *E. coli* DH5α was more sensitive than *Bacillus subtilis* and *Streptococcus aureus* for the toxicity of metal oxide nanoparticles. Furthermore, generally, *E. coli* DH5α was used for toxicity experiments in the literature (Verma et al., 2008; Baek and An, 2011; Cai et al., 2019). Thus, in this study, *E. coli* DH5α was selected as the model bacteria to be use in toxicity experiments. The toxic effects of HPs and their reaction products were assessed considering the inhibition of growth of selected bacteria. *E. coli* DH5α was grown in a Luria-Bertani (LB) culture medium (10 mL) at 37 °C, with constant shaking at 150 rpm overnight. Then, the cultures were diluted (1:10) into 100 mL media and grown under the same conditions. At the point where the optical density (OD) of bacterial cultures reached about 0.8 at 600 nm, 10 mM HPs and their enzymatic reaction products were added to the cultures and subsequently incubated at 37 °C, 150 rpm for 24 h. The assays were carried out in a cuvette (1 mL). At the end of 24 h-incubation with and without pollutants, the growth of bacteria was monitored via absorbance readings at 600 nm with a UV–Vis spectrophotometer. The growth inhibition was evaluated by comparing the differences between the absorbance values of the samples with pollutants and those of control samples at 0 h and 24 h. Experiments for control 1 (LB and acetonitrile) and control 2 (LB and KPi buffer solution) samples were conducted within the same period of time.

2.9. Analytical methods

The GC data were analyzed by SHIMADZU GC-2010 Pro equipped with CP-Sil 8 CB GC column (25 m × 0.25 mm × 1.2 μm). The oven was programmed to 90 °C for 7 min, and then its temperature was raised to 345 °C at a rate of 15 °C/min and held for 1 min at 345 °C. GC-MS analyses were performed to determine the products formed through the enzymatic reaction. A Shimadzu GC-2010 system which was connected to the GCMS-QP2010s mass detector from Shimadzu was utilized in the presence of CP-Sil 5 CB GC column (25 m × 0.25 mm × 0.4 µm). Conversion of HPs to products was determined based on calibration curves established using internal standards.

3. Results and discussion

3.1. Enzyme characteristics

The SDS Page analysis indicated that purification process was successful (Fig. S1). There was a band between 37 and 50 kDa (Fig. S1). The analysis results were consistent with the findings in the literature. For instance, Carballares et al. (2021) conducted an SDS-PAGE analysis to evaluate the expression and homogeneity of the r*Aae*UPO from *Agrocybe aegerita.* They observed a SDS band between 30 kDa and 45 kDa.

The activity and concentration of r*Aae*UPO were calculated to be 9612 U/mL and 20.7 mg/L, respectively. The characteristic shift of the Soret peak from 420 to 442 and 446 nm when CO binds to the reduced heme cofactor is seen in Fig. S2. Based on the abundance of the peak at 450 nm, the concentration of r*Aae*UPO was estimated to be 250 µM.

3.2. Molecular docking results

Molecular docking protocol was performed to predict the binding affinities of HPs to r*Aae*UPO. The corresponding docking results were shown in Fig. S3 and Table S1 and detailed in SM. In both AutoDock Vina and DockThor Programs, the binding affinity of HPs to r*Aae*UPO was 4-CP< 4-BP< 3-CP< 2-CP< 3-IP. These differences in predicted binding affinities may be attributed to variations in substrate binding orientation within the active-site cavity of r*Aae*UPO. In particular, 3-IP displayed a more favorable orientation of its aromatic ring toward the Phe triad (Phe69, Phe121, and Phe199), which has been reported to play an important role in stabilizing and properly orienting aromatic substrates in *Aae*UPO through hydrophobic and π–π stacking interactions (Molina-Espeja et al., 2014). Such an orientation may facilitate stronger non-covalent interactions between the ligand and the enzyme, thereby enhancing substrate stabilization within the catalytic pocket. Furthermore, the iodine substituent present in 3-IP possesses a larger van der Waals radius and greater electronic polarizability than other halogens such as chlorine and bromine. These physicochemical properties can enhance dispersion forces and hydrophobic contacts within the enzyme binding pocket, potentially leading to stronger ligand–protein interactions (Auffinger et al., 2004). In contrast, p-substituted compounds such as 4-CP exhibited a slightly less favorable binding orientation with respect to the catalytic residues (Arg189 and Glu196) which are implicated in peroxide activation and substrate oxidation in UPOs. Such suboptimal alignment may weaken productive enzyme–substrate interactions and contribute to the lower predicted binding affinity. Overall, the docking analysis suggests that both the substitution pattern on the aromatic ring and the size and physicochemical properties of the halogen substituent significantly influence substrate binding orientation and interaction strength within the r*AaeUPO* active site. These structural factors likely contribute to the observed differences in predicted binding affinities among the investigated HPs (Auffinger et al., 2004; Molina-Espeja et al., 2014).

3.3. Enzymatic reactions of HPs

Pioneering work by Karich et al. (2017) indicated that r*Aae*UPO could be a suitable catalyst. Considering the reactivity pattern of r*Aae*UPO with aromatic substrates (Karich et al., 2013; Gomez de Santos et al., 2018; Gomez de Santos et al., 2019; Zhang et al., 2021), selective *ortho*-hydroxylation (with respect to the pre-existing hydroxyl group) was assumed to represent the first step of r*Aae*UPO-mediated degradation (Fig. 1).

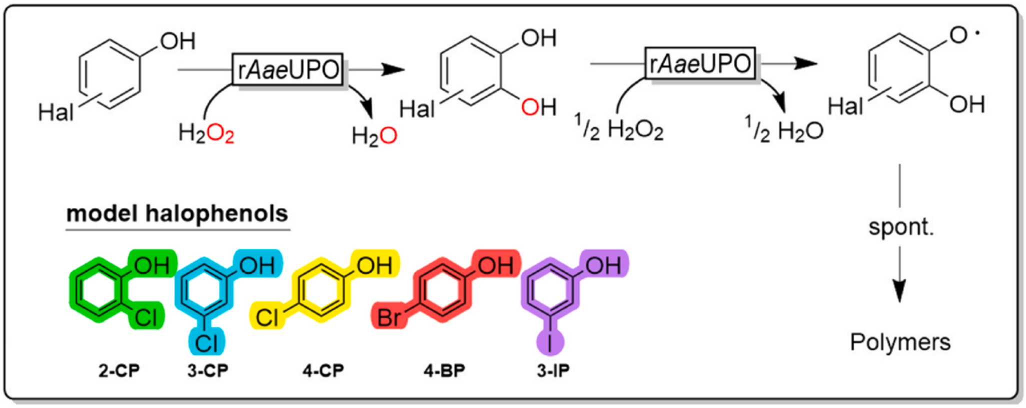

Fig. 1. Proposed detoxification mechanism of halophenols initiated by r*Aae*UPO-catalyzed hydroxylation and H-atom abstraction followed by spontaneous polymerization.

3.3.1. *Influence of reactant concentrations on HP removal*

In the first set of experiments, the impact of catalyst, pollutant, and H_2O_2concentrations on the efficiency of HP oxidation was investigated. It is worth noting that in the absence of H_2O_2 or r*Aae*UPO, only a slight reduction in the HP concentration was detected at the beginning. This may be due to the adhesion of the HPs to the vessel walls. As seen in Fig. 2a, an increase in the enzyme concentration resulted in increasing HP removal rates. When the enzyme concentration in the reaction mixture was raised from 0 to 5 μM in the presence of 25 mM H_2O_2, the concentrations of 2-CP, 3-CP, 4-CP, 4-BP, and 3-IP were reduced from 2.5 mM to below 1 mM within 30 min. Nevertheless, raising the enzyme concentration from 2.5 μM to 5 μM did not significantly enhance the removal efficiency. On the other hand, further increasing the H_2O_2 concentration led to a gradual improvement in HP removal efficiency (Fig. 2b). This is because increasing the H_2O_2 concentration initially enhanced the activity of UPOs by providing more oxidants for catalysis. However, as the H_2O_2 concentration exceeded 25 mM in the reaction solution, there was a decrease in most of the HPs' removal efficiency. That is, the high H_2O_2 concentration can lead to the formation of reactive oxygen species, resulting in heme bleaching or oxidative inactivation of the enzyme. Therefore, the H_2O_2 concentration in the batch system was set to 25 mM for the time-course experiments of r*Aae*UPO-catalyzed HP conversions. Interestingly, the theoretical H_2O_2-to-HP stoichiometry was not met in any of these experiments. This can be attributed to the intrinsic catalase activity of r*Aae*UPO (Karich et al., 2016). An intriguing exception was 3-IP, which was completely removed from the reaction mixture even in the presence of sub-stoichiometric amounts of H_2O_2. Increasing the HP concentration resulted in incomplete degradation within the time frame of the experiment (Fig. 2c). r*Aae*UPO degraded all 2.5 mM HPs with over 95% efficiency, but less than 50% of 10 mM HPs within 30 min. This is likely due to the short reaction time (30 min). A prolonged reaction time would be necessary for higher substrate loadings.

3.3.2. *Time courses of the rAaeUPO-catalyzed HP conversions*

The kinetics of r*Aae*UPO-catalyzed oxidation of HPs were investigated under partially optimized reaction conditions both in the presence and absence of NaAsc. In the experiments without NaAsc, r*Aae*UPO degraded all HPs with 90% removal efficiency, but no distinct product formation was observed (Fig. S4). This may be due to r*Aae*UPO-catalyzed hydrogen abstraction from either the phenolic substrate or the catechol product, initiating their radical polymerization (Karich et al., 2013). There was no significant decrease in HP concentrations in all control samples without enzyme.

In this study, the degradation of HPs with NaAsc by r*Aae*UPO occurred through catechol pathway. Fragmentation ions of HPs and

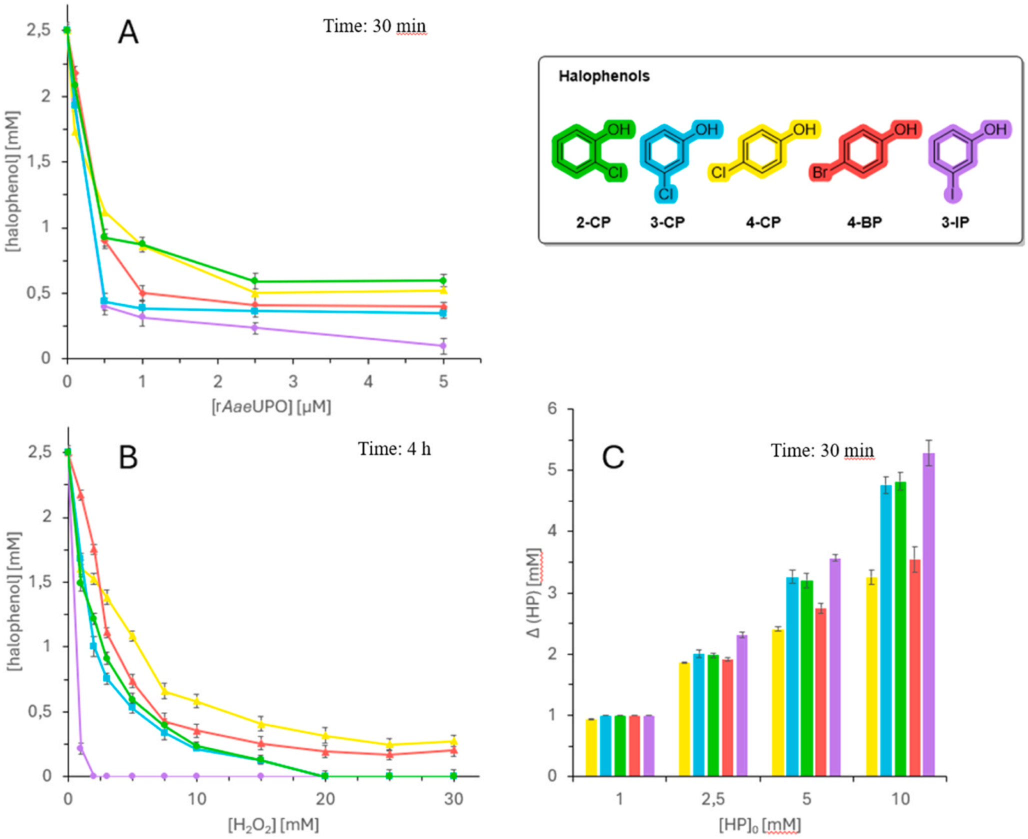

Fig. 2. Influence of the concentration of (a) enzyme, (b) H_2O_2, and (c) Halophenols on the degradation efficiency. General conditions: [r*Aae*UPO] = 5 μM (B and C), [H_2O_2] = 25 mM (A and C), $[HP]_0$ = 2.5 mM (A and B), NaAsc= 15 mg/mL, T = 30 °C, KPi buffer (50 mM, pH=7.5). (Error bars represent mean ± SD (n = 3)).

their products detected in GC-MS analysis were detailed in Figs S5 and S6 and Table S2. In the enzymatic degradation experiments conducted using 25 mM H_2O_2 in the presence of NaAsc, r*Aae*UPO also exhibited a high ability to degrade 2-CP and 3-CP within a short time. At the end of 4 h-incubation period, 2-CP was completely converted into 3-Chlorocatechol (3-CC) in the batch system (Fig. 3a). These results were confirmed by GC-MS analysis (Fig. S7b). On the other hand, r*Aae*UPO fully transformed 3-CP to 3-CC and 4-CC within 4 h (Fig. 3b and Fig. S8b). At the end of 72 h, it was able to convert 4-CP into 4-CC at a conversion rate of 89.6% (Fig. 3c and Fig. S9b). Jiang et al. (2025) reported that 1 μM CYP152 peroxygenase converted 0.5 mM 3-CP to 3-CC and 4-CC at the ortho and para positions, respectively, achieving a conversion efficiency of 52.4% in an in-situ H_2O_2-releasing system after 6 h. In contrast,

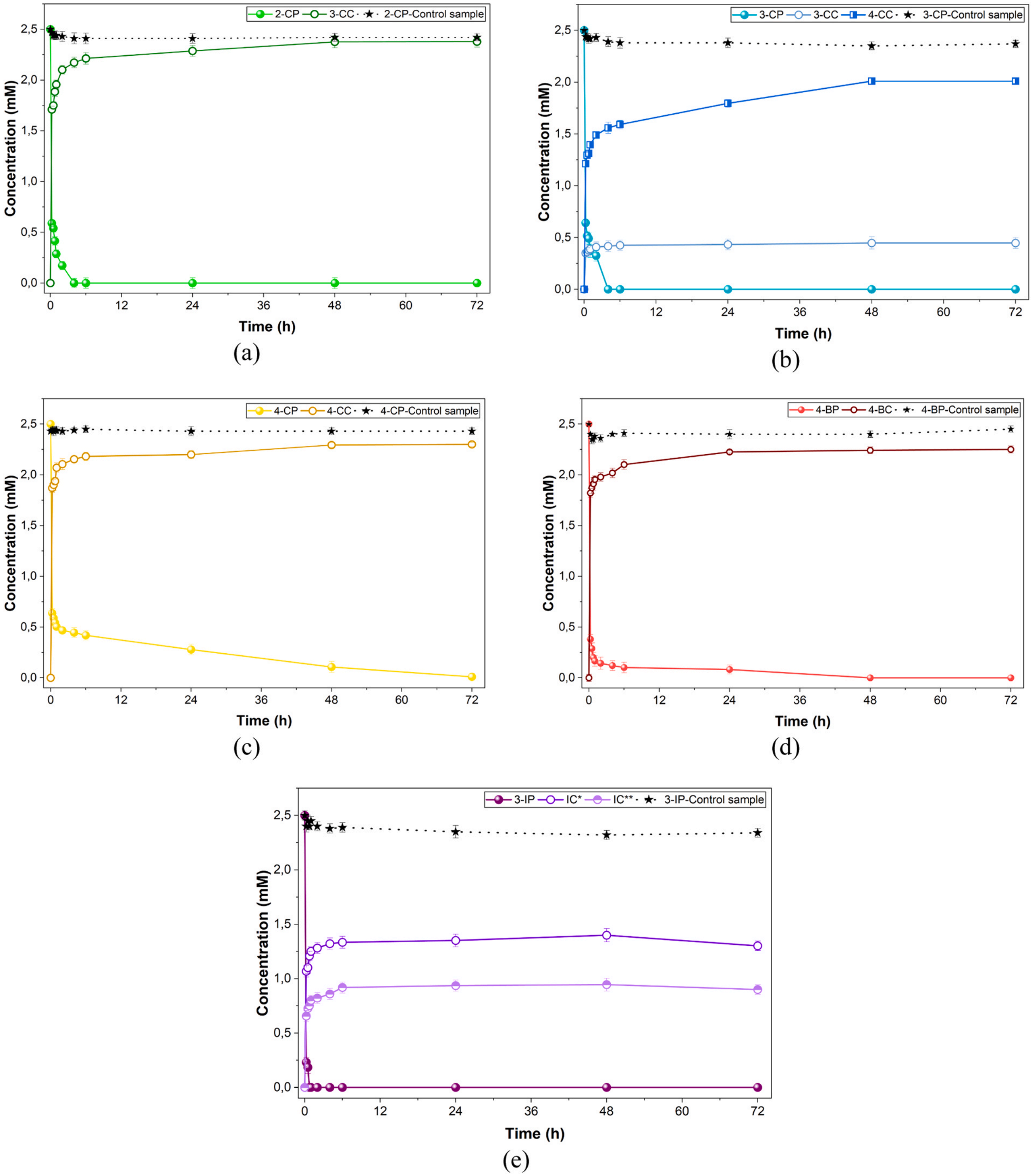

(a)

(b)

(c)

(d)

(e)

Fig. 3. Time courses of the r*Aae*UPO-catalysed halophenol degradation reactions in batch system General conditions: [r*Aae*UPO] = 5 μM, [H_2O_2] = 25 mM, $[HP]_0$ = 2.5 mM, NaAsc= 15 mg/mL, T = 30 °C, t = 72 h, KPi buffer (50 mM, pH=7.5). (Error bars represent mean ± SD (n = 3)).

hydroxylation of 0.5 mM 4-CP occurred exclusively at the ortho position (4-CC), with a conversion efficiency of 30.6%. These results are consistent with the present study.

Overall, the time-course analysis of CP degradation by the r*Aae*UPO enzyme revealed that 2-CP was transformed most rapidly, while 4-CP exhibited the slowest transformation rate. As for 4-BP degradation, the product that emerged because of the enzymatic catalysis of 4-BP was identified to be 4-Bromocatechol (4-BC) (Fig. S10b). As seen in Fig. 3e, whereas the concentration of 3-IP in the control sample did not significantly change during the entire incubation time, r*Aae*UPO enzyme fully degraded the 3-IP within 45 min with an accumulation of two different types of potential iodocatechols (ICs) in the batch system. Based on the mass data and

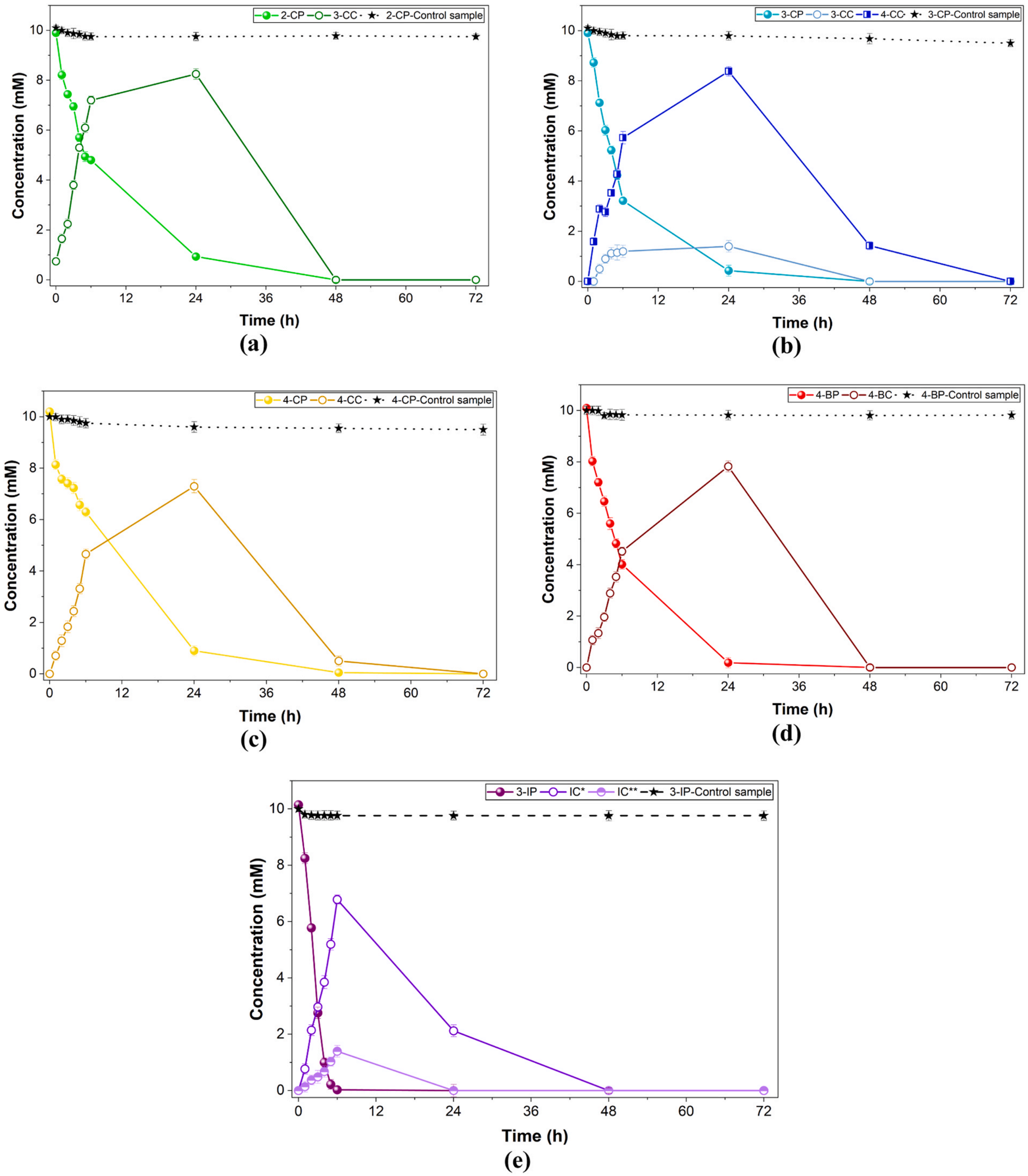

(a)

(b)

(c)

(d)

(e)

Fig. 4. Time courses of the *Aae*UPO-catalysed halophenol degradation reactions. General conditions: [r*Aae*UPO] = 5 μM, [H_2O_2] = 2 mM/h, $[HP]_0$ = 10 mM, NaAsc= 15 mg/mL, T = 30 °C, t = 72 h, KPi buffer (50 mM, pH=7.5). (Error bars represent mean ± SD (n = 3)).

fragmentation ions of 3-IC in Fig. S6d, it was determined that none of these products were 3-IC but could be other substituted ICs. These products can be isomers with 3-IC, because they exhibited the same fragmentation ions with 3-IC (Fig. S11b). At the end of 72 h, 3-IP was completely converted into its metabolites by r*Aae*UPO.

In the fed-batch experiments, to minimize oxidative inactivation of r*Aae*UPO caused by excess H_2O_2 (Burek et al., 2019), H_2O_2 was continuously supplied from a stock solution via a syringe pump. Under these conditions, the expected catechol products accumulated during the first 24 h and subsequently disappeared over the following 24 h (Fig. 4). r*Aae*UPO was able to fully convert 10 mM of all CPs and 4-BP to their corresponding catechols within 72 h in the fed-batch system (Fig. 4). However, after 24 h, the concentration of the corresponding catechols decreased, becoming undetectable after 72 h. As seen in Fig. 4e, at the end of 6 h, it entirely removed 3-IP with the accumulation of metabolites. Interestingly, in the reactions with 3-CP and 3-IP, two catechol products were formed. For 3-CP, this can be rationalized by hydroxylation at the *ortho*- and *para*- positions relative to the preexisting hydroxyl group. Nevertheless, all primary r*Aae*UPO-hydroxylation products underwent polymerization and were not detectable after 72 h latest. Consequently, these time-course profiles are consistent with the proposed reaction sequence: during the first 24 h, NaAsc acts as a sacrificial reductant, scavenging phenoxy and catechoxy radicals. However, after its depletion, polymerization removes the intermediate catechol products. The initial catechol formation rates ranged between 0.72 (with 4-BP) and 1.23 mM (with 3-IP) h^{-1} corresponding to approximately 50% of the H_2O_2 used productively. r*Aae*UPO's catalase activity may be responsible for this rather modest utilization of H_2O_2. Compared to the r*Aae*UPO's performance in batch and fed-batch systems, r*Aae*UPO could catalyze the reaction of HPs with higher concentration in the fed-batch system within the same time. This demonstrated that the enzyme was more effective in reactions fed with lower concentrations of H_2O_2. Further optimization of the oxidant feed rate can increase the H_2O_2 utilization efficiency.

Considering the time course of the entire HP degradation, r*Aae*UPO exhibited the lowest degradation rate for 4-CP, while demonstrating the highest degradation rate for 3-IP. In line with this, Davis et al. (2018) reported that the catalytic efficiency of WT tyrosinase and variant enzymes toward HPs was determined to increase with increasing substitution size ($F < Cl < Br < I$). Among the HPs, r*Aae*UPO exhibited the highest and lowest affinities towards 3-IP and 4-CP, respectively according to molecular docking results. This may be attributed to the combined effects of electronic modulation of aromatic reactivity, substituent-dependent steric control of active site alignment and intrinsic C-X bond reactivity, all within the established catalytic framework of UPO-mediated aromatic hydroxylation. r*Aae*UPO operates through the peroxide shunt pathway, forming a high-valent oxoferryl species capable of electrophilic oxygen transfer to aromatic substrates (Hofrichter and Ullrich, 2014). Halogen substituents exert an electron-withdrawing inductive effect, which decreases the electron density of the aromatic ring and influences its susceptibility toward electrophilic hydroxylation (Carey and Sundberg, 2007). Periodic trends further indicate that electronegativity decreases while polarizability increases in the

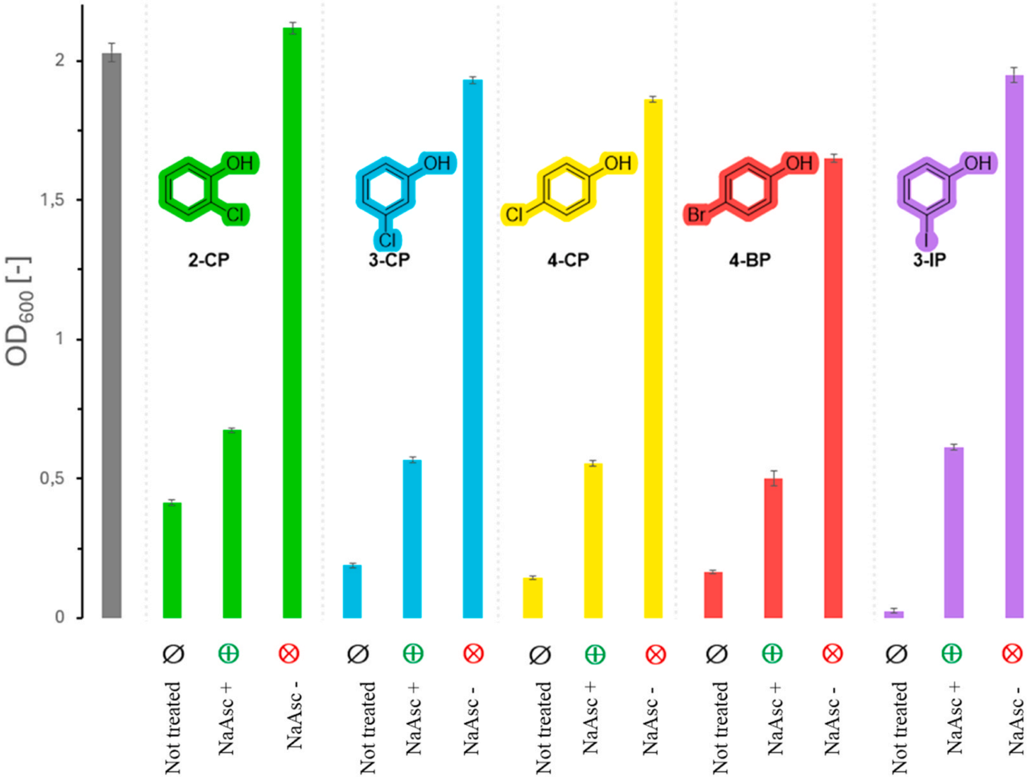

Fig. 5. Preliminary toxicity study on some halopenols treated with r*Aae*UPO. ∅: HP sample not treated, ⊕: HP sample treated with r*Aae*UPO/H_2O_2 in the presence of NaAsc, ⊗: HP sample treated with r*Aae*UPO/H_2O_2 in the absence of NaAsc. General conditions: [r*Aae*UPO] = 5 μM, [H_2O_2] = 25 mM, $[HP]_0 = 10$ mM, T = 30 °C, t = 72 h, KPi buffer (50 mM, pH=7.5). (Error bars represent mean ± SD (n = 3)).

order of F < Cl < Br < I (Atkins and de Paula, 2014). Iodine and bromine-substituted phenols, which contain halogens with higher polarizability and larger atomic radius than chlorine-substituted phenols, may experience more favorable transitation-state stabilization during electrophilic oxygen transfer. These factors together are likely to be responsible for the comparatively faster conversion of iodophenols observed experimentally. Furthermore, steric effects further influence catalytic efficiency by modulating substrate positioning within the heme active site. Differences in halogen atomic radius (I > Br > Cl) may affect the distance and orientation of the reactive carbon relative to the oxoferryl center, thereby impacting conversion efficiency of HPs. Additionally, intrinsic C-X bond strength decreases in the order of C-Cl > C-Br > C-I (Luo, 2007). The relatively weaker C-I bond may facilitate subsequent hydroxylation or oxidation steps, contributing to the more rapid conversion of iodophenols.

3.4. *Toxicity experiments*

E. coli DH5α was used as a model organism in growth experiments to determine whether the enzymatic treatment effectively reduced the cytotoxicity of HPs and to evaluate possible detoxification effects. Growing *E. coli* cultures were incubated with HP samples (final nominal concentration of 10 mM in the cultivation broth) that had been pre-treated with r*Aae*UPO/H_2O_2 both in the absence and presence of NaAsc (Fig. 5). In line with literature reports, all HPs significantly inhibited microbial growth (Fig. 5 ⊘). While 2-CP showed a smaller toxic effect than other HPs, 4-CP and 4-BP exhibited more inhibitory properties on the growth rate of *E. coli* DH5α. Likewise, Pera-Titus et al. (2004) reported 4-CP was more toxic than other CPs. Generally, 4-substituted phenols such as 4-CP and 4-BP exhibit toxic effects at high concentration (Brooks et al., 2004; Nolan and O'Connor, 2007). The results of the present toxicity experiments support and are consistent with the findings reported in the literature. These results showed that toxic effect of HPs towards *E.coli* DH5α decreases in order of 4-CP, 4-BP, 3-CP, 3-IP, and 2-CP. Interestingly, the samples treated with r*Aae*UPO/H_2O_2 in the presence of NaAsc (Fig. 5 ⊕) still showed pronounced growth inhibition, whereas the samples treated in the absence of NaAsc (Fig. 5 ⊗) reached almost the same final optical density as the positive controls. Especially the latter finding was unexpected at first sight. However, it was concluded that this was an indication that ascorbate inhibited the radical polymerization of the initial catechol products. Consequently, upon addition of the HP samples, those treated with NaAsc contained comparatively high catechol concentrations. The main detoxification mechanism of the proposed r*Aae*UPO/H_2O_2 treatment may lie in the polymerization and subsequent precipitation of the HP reagents.

4. Conclusion

This study demonstrated the efficient degradation of halophenols (HPs) by recombinant unspecific peroxygenase (r*Aae*UPO) expressed in *Pichia pastoris* under batch and fed-batch conditions. The enzyme showed high catalytic activity toward HPs through aromatic hydroxylation reactions, which was consistent with molecular docking results. Among the tested compounds, 3-IP and 2-CP were transformed more rapidly than the other substrates. The fed-batch strategy enabled the effective degradation of higher HP concentrations within shorter reaction times, while lower H_2O_2 levels were found to favor catalytic efficiency. The presence of sodium ascorbate influenced the metabolic fate of the degradation products, leading to halocatechol formation, whereas polymerization occurred in its absence. Importantly, toxicity assays using *E. coli* DH5α revealed a significant reduction in toxicity following enzymatic treatment. Overall, r*Aae*UPO can offer an effective biotechnological solution as a promising biocatalyst for the enzymatic treatment of halogenated phenolic pollutants in contaminated environments. Future studies should focus on improving enzyme stability and reusability through immobilization or protein engineering strategies, as well as evaluating the performance of r*Aae*UPO in complex environmental matrices and continuous bioreactor systems to facilitate practical environmental applications.

Ethical Approval

Not needed as the study does not involve human or animal experiments or related ethical considerations.

CRediT authorship contribution statement

Esin Balci: Writing – original draft, Investigation, Methodology, Formal analysis, Data curation, Conceptualization. **Pablo Velázquez García:** Writing – original draft, Investigation, Methodology, Formal analysis, Data curation, Conceptualization. **Miguel Alcalde:** Sources, Methodology. **Frank Hollmann:** Writing – review & editing, Methodology, Supervision, Funding acquisition, Project administration, Conceptualization.

Declaration of Competing Interest

The authors declare that they have no known competing financial interests or personal relationships that could have appeared to influence the work reported in this paper.

Acknowledgment

This study was funded by the European Union (ERC, PeroxyZyme, No 101054658). Views and opinions are expressed, however, those of the authors only and do not necessarily reflect those of the European Union or the European Research Council. Neither the

European Union nor the granting authority can be held responsible for them. Additionally, financial support was granted by the Scientific and Technological Research Council of Türkiye (TUBITAK) through the 2219-A International Postdoctoral Fellowship Program.

Appendix A. Supporting information

Supplementary data associated with this article can be found in the online version at doi:10.1016/j.eti.2026.104923.

Data availability

Data will be made available on request.

References

Acero, J.L., Piriou, P., van, Gunten, U., 2005. Kinetics and mechanisms of formation of bromophenols during drinking water chlorination: assessment of taste and odor development. Water Res. 39 (13), 2979–2993. https://doi.org/10.1016/j.watres.2005.04.055.

Ashraf, H.And, Husain, Q., 2010. Studies on bitter gourd peroxidase catalyzed removal of p-bromophenol from wastewater. Desalination 262 (1-2), 267–272. https://doi.org/10.1016/j.desal.2010.05.044.

Atkins, P., de Paula, J., 2014. Atkins' Physical Chemistry, 10th ed.). Oxford University Press, Oxford, UK.

Auffinger, P., Hays, F.A., Westhof, E., Ho, P.S., 2004. Halogen bonds in biological molecules. Biophys. Comput. Biol. 101 (48), 16789–16794. https://doi.org/10.1073/pnas.040760710.

Baek, Y.-W., An, Y.-J., 2011. Microbial toxicity of metal oxide nanoparticles (CuO, NiO, ZnO, and Sb_2O_3) to *Escherichia coli*, *Bacillus subtilis*, and *Streptococcus aureus*. Sci. Total Environ. 409 (8), 1603–1608. https://doi.org/10.1016/j.scitotenv.2011.01.014.

Bagheri, H., Mohammadi, A., Salemi, A., 2004. On-line trace enrichment of phenolic compounds from water using a pyrrole-based polymer as the solid-phase extraction sorbent coupled with high performance liquid chromatography. Anal. Chim. Acta 513 (2), 445–449. https://doi.org/10.1016/j.aca.2004.03.020.

Brooks, S.J., Doyle, E.M., Hewage, C., Malthouse, J.P.G., Duetz, W., O'Connor, K.E., 2004. Biotransformation of halophenols using crude cell extracts of *Pseudomonas putida* F6. Appl. Microbiol. Biotechnol. 64, 486–492. https://doi.org/10.1007/s00253-003-1488-z.

Burek, B.O., Bormann, S., Hollmann, F., Bloh, J.Z., Holtmann, D., 2019. Hydrogen peroxide driven biocatalysis. J. Green Chem. 21 (12), 3232–3249. https://doi.org/10.1039/C9GC00633H.

Cai, X., Wang, X., Chen, Y., Wang, Y., Song, D., Gu, Q., 2019. A natural biopreservative: Antibacterial action and mechanisms of Chinese Litsea mollis Hemsl. Extract against *Esherichia coli* Dh5α and *Salmonella* spp. J. Dairy Sci. 102 (11), 9663–9673. https://doi.org/10.3168/jds.2019-16292.

Carballares, D., Morellon-Sterling, R., Xu, X., Hollmann, F., Fernandez-Lafuente, R., 2021. Immobilization of the peroxygenase from *Agrocybe aegerita*. The effect of the immobilization pH on the features o fan ionically exchanged dimeric peroxygenase. Catalysts 11 (5), 560. https://doi.org/10.3390/catal11050560.

Carey, F.A., Sundberg, R.J., 2007. Advanced Organic Chemistry: Part A: Structure and Mechanisms, 5th ed.). Springer, New York.

Davis, R., Molloy, S., Quigley, B., Nikodinovic-Runic, J., Solano, F., O'Connor, R.E., 2018. Biocatalytic versatility of engineered and wild-type tyrosinase from *R. solanacearum* for the synthesis of 4-halocatechols. Appl. Microbiol. Biotechnol. 102, 5121–5131. https://doi.org/10.1007/s00253-018-8994-5.

De Boer, S., Sastre, D., Castillo, A., Balboa Mendez, S., Hollmann, F., Lores, M., Schaffer, A., Moreira, M.T., 2025. Advancing the enzymatic removal of antibiotics with unspecific peroxygenase and vanadium chloroperoxidase. J. Environ. Chem. Eng. 13, 115795. https://doi.org/10.1016/j.jece.2025.115795.

Duran, N., Esposito, E., 2000. Potential applications of oxidative enzymes and phenoloxidase-like compounds in wastewater and soil treatment: a review. Appl. Catal. B Environ. 28 (2), 83–99. https://doi.org/10.1016/S0926-3373(00)00168-5.

Gomez de Santos, P., Canellas, M., Tieves, F., Younes, S.H.H., Molina-Espeja, P., Hofrichter, M., Hollmann, F., Guallar, V., Alcalde, M., 2018. Selective synthesis of the human drug metabolite 5′-hydroxypropanolol by an evolved self -sufficient peroxygenase. ACS Catal. 8 (6), 4789–4799. https://doi.org/10.1021/acscatal.8b01004.

Gomez de Santos, P., Cervantes, F.V., Tieves, F., Plou, F.C., Hollmann, F., Alcalde, M., 2019. Benchmarking of laboratory evolved unspecific peroxygenases for the synthesis of human drug metabolites. Tetrahedron 75 (13), 1827–1831. https://doi.org/10.1016/j.tet.2019.02.013.

Hofrichter, M., Ullrich, R., 2014. Oxidations catalyzed by fungal peroxygenases. Curr. Opin. Chem. Biol. 19, 116–125. https://doi.org/10.1016/j.cbpa.2014.01.015.

Igbinosa, E.O., Odjadjare, E.E., Chigor, V.N., Igbinosa, I.H., Emoghene, A.O., Ekhaise, F.O., Igichon, N.O., Idemudia, O.G., 2013. Toxicological profile of chlorophenols and their derivatives in the environment: the public health perspective. Sci. World J., 460215 https://doi.org/10.1155/2013/460215.

Jankowska, K., Su, Z., Zdarta, J., Skiadas, I.V., Woodley, J.M., Pinelo, M., 2024. High performance removal of chlorophenols from an aqueous solution using an enzymatic membrane bioreactor. Environ. Pollut. 357, 124348. https://doi.org/10.1016/j.envpol.2024.124348.

Jiang, J., Gao, Y., Pang, S.Y., Wang, Q., Xuangfu, X., Liu, Y., Ma, J., 2014. Oxidation of bromophenols and formation of brominated polymeric products of concern during water treatment with potassium permanganate. Environ. Sci. & Technol. 48 (18), 10850–10858. https://doi.org/10.1021/es5008577.

Jiang, Y., Gong, P., Li, Z., Wang, B., Huang, H., Peng, W., Gao, X., Li, S., 2025. Unexpected activities of CYP152 peroxygenases toward non-carboxylic substrates reveal novel substrate recognition mechanism and catalytic versatility. Angew. Chem. 64 (31), e202506614. https://doi.org/10.1002/anie.202506614.

Kang, C., Yang, J.W., Cho, W., Kwak, S., Park, S., Lim, Y., Choe, J.W., Kim, H.S., 2017. Oxidative biodegradation of 4-chlorophenol by using recombinant-monooxygenase cloned and overexpressed from Arthrobacter chlorophenolicus A6. Bioresour. Technol. 240, 123–129. https://doi.org/10.1016/j.biortech.2017.03.078.

Karich, A., Kluge, M., Ullrich, R., Hofrichter, M., 2013. Benzene oxygenation and oxidation by peroxygenase of Agrocybe aegerita. AMB Express 3, 5. https://doi.org/10.1186/2191-0855-3-5.

Karich, A., Scheibner, K., Ullrich, R., Hofrichter, M., 2016. Exploring the catalase activity of unspecific peroxygenases and the mechanism of peroxide-dependent heme destruction. J. Mol. Catal. B Enzym. 134 (A), 238–246. https://doi.org/10.1016/j.molcatb.2016.10.014.

Karich, A., Ullrich, R., Scheibner, K., Hofrichter, M., 2017. Fungal unspecific peroxygenases oxidize the majority of organic EPA priority pollutants. 8, 1403. https://doi.org/10.3389/fmicb.2017.01463.

Kim, H.J., Suma, Y., Lee, S.H., Kim, J.A., Kim, H.S., 2012. Immobilization of horseradish peroxidase onto clay minerals using soil organic matter for phenol removal. J. Mol. Catal. B Enzym. 83, 8–15. https://doi.org/10.1016/j.molcatb.2012.06.012.

Lin, K., Song, L., Zhou, S., Chen, D., Gan, J., 2016. Formation of brominated phenolic contaminants from natural manganese oxides-catalyzed oxidation of phenol in the presence of Br^-. Chemosphere 155, 266–273. https://doi.org/10.1016/j.chemosphere.2016.04.064.

Liu, J., Liu, Y., Tian, Y., Feng, L., Zhang, L., 2020. Comparison of the oxidation of halogenated phenols in UV/PDS and UV/H_2O_2 advanced oxidation processes. RSC Adv. 10, 6464–6472. https://doi.org/10.1039/C9RA10401A.

Loncar, N., Bozic, N., Andelkovic, I., Milovanovic, A., Dojnov, B., Vujcic, M., Roglic, G., Vujcic, Z., 2011. Removal of aqueous phenol and phenol derivatives by immobilized potato polyphenol oxidase. J. Serb. Chem. Soc. 76 (4), 513–522. https://doi.org/10.2298/JSC100619046L.

Lu, J., Shao, J., Liu, H., Wang, Z., Huang, Q., 2015. Formation of halogenated polyaromatic compounds by laccase-catalyzed transformation of halophenols. Environ. Sci. & Technol. 49, 8550–8557. https://doi.org/10.1021/acs.est.5b02399.

Luo, Y.R., 2007. Comprehensive Handbook of Chemical Bond Energies. CRC press. https://doi.org/10.1201/9781420007282.

Molina-Espeja, P., Garcia-Ruiz, E., Gonzalez-Perez, D., Ullrich, R., Hofrichter, M., Alcalde, M., 2014. Directed Evolution of Unspecific Peroxygenase from Agrocybe aegerita. Appl. Environ. Microbiol. 80 (11), 3496–3507. https://doi.org/10.1128/aem.00490-14.

Molina-Espeja, P., Ma, S., Mate, D.M., Ludwig, R., Alcalde, M., 2015. Tandem-yeast expression system for engineering and producing unspecific peroxygenase. Enzym. Microb. Technol. 73-74, 29–33. https://doi.org/10.1016/j.enzmictec.2015.03.004.

Nolan, L.C., O'Connor, K.E., 2007. Use of *Pseudomonas mendocina*, or recombinant *Escherichia coli* cells expressing toluene-4-monooxygenase, and a cell-free tyrosinase for the synthesis of 4-fluorocatechol from fluorobenzene. Biotechnol. Lett. 29, 1045–1050. https://doi.org/10.1007/s10529-007-9365-y.

Olaniran, A.O., Igbinosa, E.O., 2011. Chlorophenols and other related derivatives of environmental concern: properties, distribution, and microbial degradation processes. Chemosphere 83, 1297–1306. https://doi.org/10.1016/j.chemosphere.2011.04.009.

Pera-Titus, M., Garcia-Molina, V., Banos, M.A., Gimenez, J., Esplugas, S., 2004. Degradation of chlorophenols by means advanced oxidation processes: a general review. Appl. Catal. B Environ. 47 (4), 219–256. https://doi.org/10.1016/j.apcatb.2003.09.010.

Ra, J.S., Oh, S.Y., Lee, B.C., Kim, S.D., 2008. The effect of suspended particles coated by humic acid on the toxicity of pharmaceuticals, estrogens, and phenolic compounds. Environ. Int. 34, 184–192. https://doi.org/10.1016/j.envint.2007.08.001.

Suma, Y., Lim, H., Kwean, O.S., Cho, S., Yang, J., Kim, Y., Kang, C.S., Kim, H.S., 2016. Enzymatic degradation of aromatic hydrocarbon intermediates using a recombinant dioxygenase immobilized onto surfactant-activated carbon nanotube. Bioresour. Technol. 210, 117–122. https://doi.org/10.1016/j.biortech.2016.01.018.

Tonin, F., Tieves, F., Willot, S., van Troost, A., van Oosten, R., Breestraat, S., van Pelt, S., Alcade, M., Hollmann, F., 2021. Pilot-scale production of peroxygenase from *Agrocybe aegerita*. Org. Process Res. & Dev. 25 (6), 1414–1418. https://doi.org/10.1021/acs.oprd.1c00116.

Ullrich, R., Nüske, J., Scheibner, K., Spantzel, J., Hofrichter, M., 2004. Novel haloperoxidase from the Agaric Basidiomycete Agrocybe aegerita oxidizes aryl alcohols and aldehydes. Appl. Environ. Microbiol. 70 (8), 4575–4581. https://doi.org/10.1128/AEM.70.8.4575-4581.2004.

Verma, K., Agrawal, N., Misra, R.B., Farooq, M., Hans, R.K., 2008. Phototoxicity assessment of drugs and cosmetic products using *E. coli*. Toxicol. Vitr. 22 (1), 249–253. https://doi.org/10.1016/j.tiv.2007.08.009.

Wang, B., Gao, J., Xu, J., Han, H., Li, Z., Wang, L., Zhang, F., Tian, Y., Peng, R., Yao, Q., 2021. Optimization and reconstruction of two new complete degradation pathways for 3-chlorocatechol and 4-chlorocatechol in *Escherichia coli*. J. Hazard. Mater. 419, 126428. https://doi.org/10.1016/j.jhazmat.2021.126428.

Zhang, W., Li, H., Younes, S.H.H., Gomez de Santos, P., Tieves, F., Grogan, G., Pabst, M., Alcalde, M., Whitwood, A.-C., Hollmann, F., 2021. Biocatalytic aromaticity-breaking epoxidation of naphthalene and nucleophilic ring-opening reactions. ACS Catal. 11 (5), 2644–2649. https://doi.org/10.1021/acscatal.0c05588.